Further work will be required to fully evaluate the effect of the inductive reactance, together with its compensations, in microstrip and stripline designs of impedance transformers and filters.

References

[1] A. A. Oliner, "Equivalent circuit for discontinuities in balanced strip transmission line," *IRE Trans. Microwave Theory Tech. (Special Issue on Microwave Strip Circuits)*, vol. MTT-3, pp. 134–143, Mar. 1955.
[2] J. R. Whinnery and H. W. Jamieson, "Equivalent circuits for discontinuities in transmission lines," *Proc. IRE*, vol. 32, pp. 98–114, Feb. 1944.
[3] R. E. Collin, *Field Theory of Guided Waves*. New York: McGraw-Hill, 1960.
[4] J. Schwinger and D. S. Saxon, *Discontinuities in Waveguides*. New York: Gordon and Breach, 1968.
[5] H. M. Altschuler and A. A. Oliner, "Discontinuities in the center conductor of symmetric strip transmission line," *IRE Trans. Microwave Theory Tech.*, vol. MTT-8, pp. 328–339, May 1960.
[6] L. Weinberg, *Network Analysis and Synthesis*. New York: McGraw-Hill, 1962, sec. 2.1.

Waveguides of Arbitrary Cross Section by Solution of a Nonlinear Integral Eigenvalue Equation

BARRY E. SPIELMAN, MEMBER, IEEE, AND ROGER F. HARRINGTON, FELLOW, IEEE

***Abstract*—The problem of electromagnetic wave propagation in hollow conducting waveguides of arbitrary cross section is formulated as an integro-differential equation in terms of fields at the waveguide boundary. Cutoff wave numbers and wall currents appear as eigenvalues and eigenfunctions of a nonlinear eigenvalue problem involving an integro-differential operator. A variational solution is effected by reducing the problem to matrix form using the method of moments.**

A specific solution of the problem is developed using triangle expansion functions in the method of moments. The solution is simplified by symmetry considerations and is implemented by two digital computer programs. Listings and full documentation of these programs are available. This solution yields accurate determinations of cutoff wave numbers, wall currents, and distributions of both longitudinal and transverse modal field components for the first several modes. Illustrative computations are presented for the single-ridge waveguide, which has a complicated boundary shape that does not lend itself to exact solution.

I. Introduction

ELECTROMAGNETIC wave propagation in hollow conducting waveguides of arbitrary cross section is a problem of considerable interest. An interesting review paper by Davies [1] gives a comparative discussion of many of the methods previously applied to this general problem. His discussion makes clear that no single solution method has proved to be best for all requirements that might be imposed.

In this paper a new solution for waveguides of arbitrary cross section is presented. The approach is based on an integral operator formulation which affords a unified treatment of the various classes of waveguide shape. In principle, the first several modes can be analyzed provided the boundary of the waveguide is closed. The convergence characteristics and accuracy of the method have been demonstrated previously [2]. Example calculations of cutoff wave numbers and field distributions are presented here for modes of the single-ridge waveguide.

Manuscript received November 1, 1971; revised April 10, 1972.
B. E. Spielman is with the Naval Research Laboratory, Washington, D. C.
R. F. Harrington is with Syracuse University, Syracuse, N. Y.

II. Integral Formulation

The problem is formulated as follows. For waveguides containing only a homogeneous isotropic medium, the electric field within the waveguide is expressed in terms of the vector potential A and scalar potential ϕ as

$$E = -j\omega A - \nabla\phi \tag{1}$$

where

$$A = \mu \oint_C JG(kR)dl \tag{2}$$

$$\phi = \frac{1}{\epsilon} \oint_C \sigma G(kR)dl. \tag{3}$$

Here, $G(kR)$ is the two-dimensional Green's function and can be expressed in terms of $H_0^{(2)}$, the Hankel function of the second kind zero order as

$$G(kR) = \frac{1}{4j} H_0^{(2)}(kR). \tag{4}$$

Also, C is the contour bounding the waveguide cross section, dl is the element of arc along C, R is the distance between a source point and the field point, k is the wave number, and μ and ϵ are the permeability and permittivity of the medium within the waveguide. The quantities J and σ are the wall current and charge, respectively, related by the equation of continuity. The

boundary condition is expressed as

$$\boldsymbol{E}_{\tan} = 0 \tag{5}$$

where tan denotes the tangential component of electric field on C. The problem can now be stated succinctly as

$$L(J) = 0 \tag{6}$$

where L is the integro-differential operator

$$L(J) = -\boldsymbol{E}_{\tan} = [j\omega \boldsymbol{A} + \nabla\phi]_{\tan}. \tag{7}$$

Solution of (6) gives cutoff wave numbers $\{k_n\} = \{k_1, k_2, \cdots\}$ and corresponding wall currents, $\{J_n\} = \{J_1, J_2, \cdots\}$, on C. The modal fields are functions of $\{J_n\}$ and can be computed once the currents are known.

III. Reduction to Matrix Formulation

The determination of waveguide cutoff wave numbers and wall currents requires the solution of (7) subject to the boundary condition in (5). To facilitate such a solution, (7) is reduced to matrix form by the method of moments, which is closely related to Galerkin's method [3], [4].

A. Method of Moments Reduction

For the method of moments, define the inner product

$$\langle \boldsymbol{W}, \boldsymbol{J} \rangle = \oint_C \boldsymbol{W} \cdot \boldsymbol{J} dl \tag{8}$$

where the vectors $\boldsymbol{W}$ and $\boldsymbol{J}$ are tangential to C. A set of expansion functions $\{J_n\}$ is chosen and the current on C is expanded as

$$\boldsymbol{J} = \sum_n I_n \boldsymbol{J}_n. \tag{9}$$

Using this expansion for $\boldsymbol{J}$ and invoking the linearity of the operator L in (7)

$$\sum_n I_n L(J_n) = -\boldsymbol{E}_{\tan}. \tag{10}$$

A set of testing functions $\{\boldsymbol{W}_m\}$ is now chosen such that each $\boldsymbol{W}_m$ is tangential to C. Taking the inner product of each $\boldsymbol{W}_m$ with (10) yields

$$\sum_n I_n \langle \boldsymbol{W}_m, L(J_n) \rangle = \langle \boldsymbol{W}_m, -\boldsymbol{E} \rangle \tag{11}$$

for $m = 1, 2, \cdots$. Equation (11) can be written as the generalized network matrix equation

$$[Z][I] = [V] \tag{12}$$

which upon application of the boundary condition in (5) becomes

$$[Z][I] = [0]. \tag{13}$$

The present form of the elements in the impedance matrix is

$$z_{mn} = \oint_C \boldsymbol{W}_m \cdot (j\omega \boldsymbol{A}_n + \nabla\phi_n) dl. \tag{14}$$

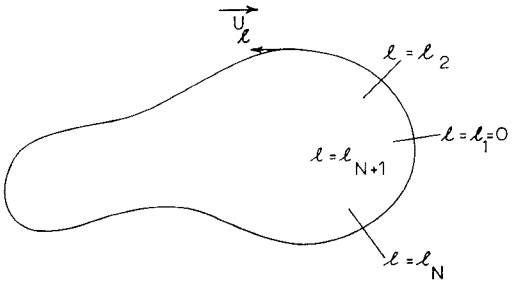

Fig. 1. Details of the contour subdivision.

The subscript n denotes that $\boldsymbol{A}_n$ and ϕ_n are potentials due to J_n and σ_n. Applying the one-dimensional form of the divergence theorem to $\phi_n \boldsymbol{W}_m$, (14) is transformed to the computationally advantageous form [2]

$$z_{mn} = j\omega \oint_C (\boldsymbol{W}_m \cdot \boldsymbol{A}_n + \sigma_m \phi_n) dl \tag{15}$$

where σ_m is defined as

$$\sigma_m = -\frac{1}{j\omega} \nabla \cdot \boldsymbol{W}_m. \tag{16}$$

To this point the matrix formulation is completely general and was achieved without reference to TE or TM mode characteristics. The wall current for TE modes at cutoff is two-dimensional and circumferentially directed. For such a current the impedance element form in (15) is suitable.

However, for TM modes at cutoff the wall current is two-dimensional, axially directed, and hence divergenceless. It follows that the impedance element in (15), for TM modes, becomes

$$z_{mn} = j\omega \oint_C \boldsymbol{W}_m \cdot \boldsymbol{A}_n dl. \tag{17}$$

In the following sections, specific expansion and testing functions are used with (15) and (17) to effect solutions for TE and TM modes, respectively.

B. TE Matrix Elements

The TE mode impedance matrix elements, expressed by (15), can be cast into a form convenient for computation by first writing the element in greater detail as

$$z_{mn} = \oint_C dl' \oint_C dl \left[j\omega\mu \boldsymbol{W}_m \cdot \boldsymbol{J}_n + \frac{1}{j\omega\epsilon} (\nabla' \cdot \boldsymbol{W}_m)(\nabla \cdot \boldsymbol{J}_n) \right] \cdot \frac{H_0^{(2)}(kR)}{4j}. \tag{18}$$

Here, the unprimed symbols dl and ∇ refer to source location variation, while the corresponding primed symbols relate to variation in field point location.

A specific formulation evolves by dividing the contour C into N segments, not necessarily equal in length. The end points of these segments are defined by a set of $(N+1)$ parameters $\{l = l_1 = 0, l = l_2, \cdots, l = l_{N+1}\}$, as shown in Fig. 1. Here, l is the path length proceeding

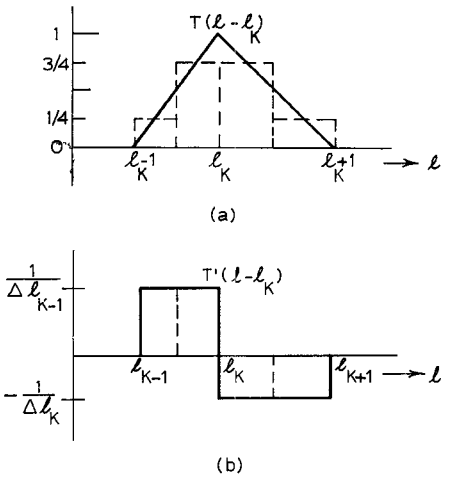

Fig. 2. (a) Triangle function. (b) Derivative of triangle function with pulse approximations indicated by broken lines.

counterclockwise around the contour C from any convenient reference point $l=l_1=0$.

The sets of expansion and testing functions are chosen as triangle functions. It is known that subsectional expansions using pulse or triangle functions give well-conditioned matrices [3]. Triangle functions were chosen for use here since the current will be differentiated to obtain the charge. Furthermore, it has been determined empirically that a triangle function expansion yields computed wave numbers which converge to exact values about twice as fast as those computed using a pulse function expansion. The triangle expansion and testing functions are defined as

$$J_k = W_k = T(l - l_k)\boldsymbol{u}_l, \qquad k = 1, 2, \cdots, N \quad (19)$$

where T is the triangle function represented by a solid line in Fig. 2(a). Also, $\boldsymbol{u}_l$ is the unit vector in the direction of increasing parameter l and is tangent to C at path length value l. Now z_{mn} can be written as

$$z_{mn} = \int_{l_{m-1}}^{l_{m+1}} dl' \int_{l_{n-1}}^{l_{n+1}} dl \left[j\omega\mu T(l' - l_m)T(l - l_n)(\boldsymbol{u}_{l'} \cdot \boldsymbol{u}_l) + \frac{1}{j\omega\epsilon} T'(l' - l_m)T'(l - l_n) \frac{H_0^{(2)}(kR)}{4j} \right] \quad (20)$$

where T' is the derivative of a triangle function and is represented by the solid line in Fig. 2(b).

The evaluation of the integrals in (20) is facilitated by making the following approximations. The triangle functions are approximated by four pulses with amplitudes $\frac{1}{4}$, $\frac{3}{4}$, $\frac{3}{4}$, $\frac{1}{4}$, as shown in Fig. 2(a). The derivative T' of the triangle function is represented exactly by four pulses with the amplitudes $1/\Delta l_{k-1}$, $1/\Delta l_{k-1}$, $-1/\Delta l_k$, $-1/\Delta l_k$, as is illustrated in Fig. 2(b). For the nth expansion function, the index $p=1, 2, 3, 4$ designates the four pulse intervals, respectively, for increasing path length. Similarly, the index $q=1, 2, 3, 4$ is assigned to the mth testing function.

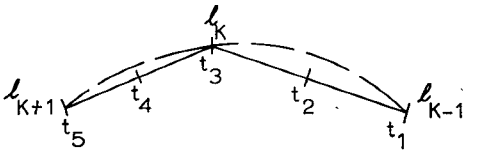

Fig. 3. Straight-line representation of the waveguide contour.

Consider the contour interval spanned by the kth expansion or testing function, as is shown in Fig. 3. In this figure the actual contour interval is indicated by a broken line. The evaluation is facilitated by defining the quantities depicted in Fig. 3.

The portion of the actual waveguide contour, represented by a broken line in the same figure, is effectively replaced by these straight lines for the evaluation of the integrals. Furthermore, define the additional quantities

$$\Delta t_k = t_{k+1} - t_k, \qquad k = 1, 2, 3, 4 \quad (21)$$

$$T_k = \begin{cases} 1/4, & k = 1, 4 \\ 3/4, & k = 2, 3 \end{cases} \quad (22)$$

$$T_k' = \begin{cases} \dfrac{-1}{\Delta l_k}, & l_k \le l \le l_{k+1} \\ \dfrac{1}{\Delta l_{k-1}}, & l_{k-1} \le l < l_k. \end{cases} \quad (23)$$

As is shown in detail elsewhere [2], the TE mode impedance element is given in final form by

$$z_{mn} = \frac{1}{16\omega\epsilon} \sum_{p,q=1}^{4} [4(k\Delta t_q)(k\Delta t_p)T_qT_p(\boldsymbol{u}_q \cdot \boldsymbol{u}_p) \mp 1]G_{qp} \quad (24)$$

where for coincident pulse intervals

$$G_{qp} = 1 - j\frac{2}{\pi} \log \frac{\gamma k\Delta t_p}{8e}. \quad (25)$$

For noncoincident pulse intervals

$$G_{qp} = H_0^{(2)}(R_{qp}). \quad (26)$$

In (24) the upper sign is taken for $(p, q \ge 3)$ or $(p, q \le 2)$; otherwise, the lower sign is taken. The unit vectors $\boldsymbol{u}_q$ and $\boldsymbol{u}_p$ are parallel to the qth and pth straight-line segments representing the qth and pth straight-line segments representing the qth and pth pulse intervals, respectively. Δt_p and Δt_q are determined by

$$\Delta t_k = t_{k+1} - t_k, \qquad k = 1, 2, 3, 4 \quad (27)$$

and R_{qp} is the distance between the centers of the qth and pth pulse intervals. The remaining quantities γ and e in (25) are the natural logarithm of Euler's constant and the natural logarithm base, respectively. It is significant that the use of (24) produces a symmetric matrix, enabling a reduction in the effort necessary in matrix calculation.

C. TM Matrix Elements

By following a procedure analogous to that used for TE mode matrix elements, the TM mode matrix elements can be written as [2]

$$z_{mn} = \frac{1}{4\omega\epsilon} \sum_{p,q=1}^{4} [(k\Delta t_p) T_q T_p] G_{qp} \tag{28}$$

where G_{qp} is defined by (25) or (26), depending on whether the source and field pulse intervals are coincident or noncoincident, respectively. The pulse amplitudes T_q and T_p are defined by (22). The interval lengths Δt_q and Δt_p are expressed by (21). The use of (28) for TM mode impedance element calculation produces a symmetric matrix with resulting computational simplification.

IV. Determination of Cutoff Wave Numbers

It has been shown [2, pp. 74–80] that the waveguide problem formulation given by (6) is a nonlinear eigenvalue problem. The cutoff wave numbers of the waveguide are the eigenvalues in this eigenvalue problem, while the wall currents are the eigenfunctions. This section sets forth the procedure used to determine these eigenvalues, while the determination of the wall currents is discussed in the next section.

Nontrivial solutions of (13) exist only if the following is true [5]:

$$|\det Z(k)| = 0. \tag{29}$$

Equation (29) will be precisely true only if the set of expansion functions used in the method of moments is complete on the domain of the operator L, given in (7). In general, the use of a finite set of expansion functions will provide only an approximation of the exact wall currents. For adequately approximated wall currents the cutoff condition is characterized by

$$|\det Z(k)| = \min. \tag{30}$$

Equation (30) has been verified for a wide variety of waveguide shapes and mode orders. Typical behavior of $|\det Z(k)|$ versus wave number is illustrated in Fig. 4. The curve shown was computed for the TE_{01} mode in a 2×1 rectangular waveguide with 12 triangle functions taken around the entire cross-section contour. The convergence of computed cutoff wave numbers towards the exact value as matrix size increases has been verified empirically and is illustrated elsewhere [2, pp. 26–29].

The evaluation of the determinant of the impedance matrix for all computations shown here was accomplished by Gauss' method [6] adapted for use on complex matrices. The determination of a minimum, satisfying (30), is made by searching $|\det Z(k)|$ as k is increased by prescribed steps. The size of these steps is reduced for successive scans of k after a minimum in $|\det Z(k)|$ is located. The step sizes have been determined by experience.

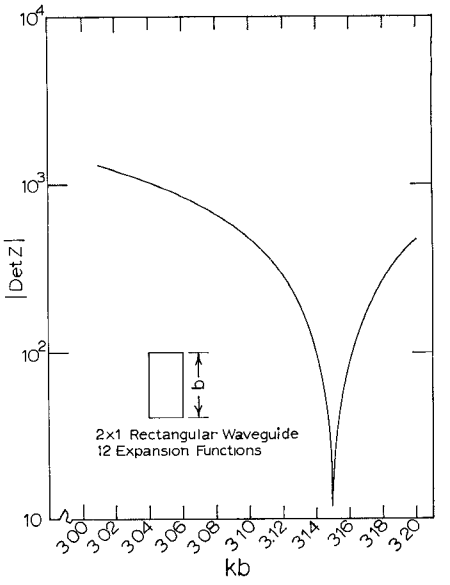

Fig. 4. Magnitude of det Z versus normalized wave number in vicinity of $TE_{0,1}$ cutoff.

V. Determination of Wall Currents

The electric and magnetic field intensities in a waveguide at cutoff are each uniform in phase over the guide cross section. It follows that the wall currents are uniform in phase about the waveguide contour. The currents are taken to be purely real around this contour. At cutoff, (13) can be separated as follows:

$$[Z][I] = [R][I] + j[X][I] = [0] \tag{31}$$

where

$$[R] = \text{Re}\,[Z] \quad \text{and} \quad [X] = \text{Im}\,[Z]. \tag{32}$$

For a complete expansion function set, (31) infers that

$$|\det X| = 0. \tag{33}$$

It follows from (33) that at least one of the eigenvalues of matrix $[X]$ is zero.

For an incomplete expansion function set, the condition in (33) becomes

$$|\det X| = \min. \tag{34}$$

Hence, an approximate wall current is an eigenvector of the matrix $[X(k)]$, corresponding to the eigenvalue of smallest modulus. The matrix $[X_c]$ is the matrix $[X]$ evaluated at a cutoff wave number determined by the method of the Section IV. Since (24) and (28) imply a symmetric impedance matrix, then the matrix $[X_c]$ is also symmetric. The eigenvalues of $[X_c]$ are therefore real quantities.

The eigenvalue problem

$$[X_c][I] = \lambda[I] \tag{35}$$

is solved numerically by using the Givens–Householder method [7]. For a waveguide with a number of degenerate or nearly degenerate modes, it is found that a

corresponding number of smallest eigenvalues are adequately computed, differing from each other by less than one order of magnitude. The computed eigenvectors corresponding to these multiple smallest eigenvalues are good approximations to the wall currents of the multiple modes.

VI. Symmetry Considerations

If a waveguide cross section is symmetrical about an axis in the transverse plane, then the problem can be reduced to two cases, one for wall currents with even symmetry about the axis and the other for currents with odd symmetry. It has been shown elsewhere [2, pp. 81–84] how significant savings in computation time and storage requirements can be achieved when such symmetries exist. For larger arrays the computation time for matrix element evaluation is reduced by nearly a factor of 2, while the time required for the solution of the eigenvalue problem is reduced by about a factor of 8.

The computations presented in this paper were done utilizing the symmetry treatment discussed in this section. The formulation prior to this section is not limited to symmetric waveguides. The method for determining field distributions, as presented next, is also not necessarily limited to symmetric waveguides.

VII. Modal Field Determination

The expressions used in the field evaluation scheme described in this paper were derived in detail in [2]. The scheme proceeds with the following consideration. Any linear measurement at a point P due to a current $\boldsymbol{J}$ about a contour C can be expressed as a linear function of $\boldsymbol{J}$, that is,

$$\text{field } (P) = \oint_C \boldsymbol{E}^r \cdot \boldsymbol{J} dl \tag{36}$$

where $\boldsymbol{E}^r$ is a known function. The current $\boldsymbol{J}$ in (36) is computed by the method discussed in Section V.

The forms taken by (36) for the rectangular coordinate modal field components are described as follows. Let a rectangular coordinate system be defined with the z axis in the direction of wave propagation. The TE and TM modal field component expressions were developed elsewhere [2, pp. 30–46, 91–95] and are described symbolically by

$$\text{field } (P) = \oint_C \left[G_1(P, l) J + G_2(P, l) \frac{dJ}{dl} \right] dl \tag{37}$$

where P is the field point. The functions G_1 and G_2 are defined in Table I for each modal field component. In this table N_0 and N_1 are the Neumann functions of order zero and one, respectively. Furthermore, (x, y) and (x', y') are the x–y coordinates of the field and source points, respectively. $\boldsymbol{u}_x$, $\boldsymbol{u}_y$, and $\boldsymbol{u}_l$ are unit vectors in the directions denoted by the subscripts.

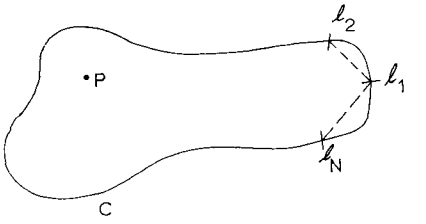

Fig. 5. Contour representation for integral evaluation.

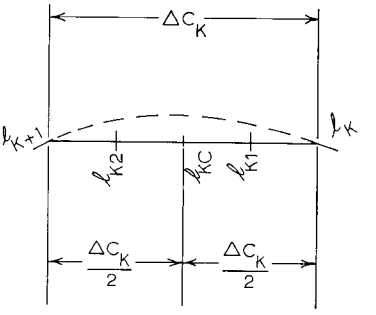

Fig. 6. kth path length interval.

TABLE I
Definitions of G_1 and G_2 for (36)

	Field	G_1	G_2
TE	H_z	$\left(-\frac{k^2}{4}\right)[(y-y')(\boldsymbol{u}_x\cdot\boldsymbol{u}_l) - (x-x')(\boldsymbol{u}_y\cdot\boldsymbol{u}_l)]\frac{N_1(kR)}{kR}$	0
	E_x	$\left(j\frac{\omega\mu}{4}\right)N_0(kR)(\boldsymbol{u}_x\cdot\boldsymbol{u}_l)$	$\left(-j\frac{\omega\mu}{4}\right)(x-x')\frac{N_1(kR)}{kR}$
	E_y	$\left(j\frac{\omega\mu}{4}\right)N_0(kR)(\boldsymbol{u}_y\cdot\boldsymbol{u}_l)$	$\left(-j\frac{\omega\mu}{4}\right)(y-y')\frac{N_1(kR)}{kR}$
TM	E_z	$\left(j\frac{\omega\mu}{4}\right)N_0(kR)$	0
	H_x	$\left(\frac{k^2}{4}\right)(y-y')\frac{N_1(kR)}{kR}$	0
	H_y	$\left(-\frac{k^2}{4}\right)(x-x')\frac{N_1(kR)}{kR}$	0

It is assumed here that the wall current $J(l)$ has been calculated at N path length values $\{l_1, l_2, \cdots, l_N\}$ around the waveguide contour by the method described in Section V. The waveguide contour C is now represented by straight-line segments drawn between adjacent path points defined by the path length values $\{l_1, l_2, \cdots, l_N\}$, as is shown in Fig. 5. The straight-line distance between adjacent path point pairs (l_1, l_2), (l_2, l_3), $\cdots$, (l_N, l_1) defines the set of lengths $\{\Delta C_1, \Delta C_2, \cdots, \Delta C_N\}$. The kth such straight-line segment is shown in Fig. 6. The current J is assumed to be linear with path length variation and is given by

$$J(l) = \frac{I_{k+1} - I_k}{\Delta C_k}(l - l_k) + I_k \tag{38}$$

where I_k and I_{k+1} are computed current values at l_k and l_{k+1}, respectively. The path length value l in (38) is taken along the straight-line segment of length ΔC_k. If P is not near the contour C, then (37) is computed assuming straight-line behavior of the integrand so that

$$\text{field } (P) = \frac{1}{2}\sum_{k=1}^{N}\left\{\begin{array}{l} G_1(P, l_{k1})J(l_{k1}) + G_1(P, l_{k2})J(l_{k2}) \\ + [G_2(P, l_{k1}) + G_2(P, l_{k2})]\dfrac{I_{k+1} - I_k}{\Delta C_k}\end{array}\right\}\Delta C_k. \quad (39)$$

Here, l_{k1} and l_{k2} are the segment midpoints shown in Fig. 6.

TE and TM mode electric field components at points near the contour C are evaluated as follows. For point P near the rth contour subdivision the electric field components are evaluated by

$$\begin{aligned}\text{field } (P) = {} & \frac{1}{2}\sum_{\substack{k=1 \\ (k\neq r)}}^{N}\left\{\begin{array}{l} G_1(P, l_{k1})J(l_{k1}) + G_1(P, l_{k2})J(l_{k2}) \\ + [G_2(P, l_{k1}) + G_2(P, l_{k2})]\dfrac{I_{k+1} - I_k}{\Delta C_k}\end{array}\right\}\Delta C_k \\ & + \frac{1}{2}\left[G_1(P, l_{r(3-i)})J(l_{r(3-i)}) + G_2(P, l_{r(3-i)})\right. \\ & \left.\cdot\frac{I_{r+1} - I_r}{\Delta C_r}\right]\Delta C_r + I_{ri}, \\ & r = 1, 2, \cdots, N \\ & i = 1, 2 \end{aligned} \quad (40)$$

where I_{ri} is developed and defined elsewhere [2, pp. 91–95], with the index i being described in the same reference. l_{r1} and l_{r2} are as shown in Fig. 6 with $k = r$.

The evaluation of the magnetic field components at points near the waveguide wall is made as follows. The TE rectangular field component H_z is given by

$$H_z(P) = J(l_{ri}), \qquad i = 1, 2 \quad (41)$$

where $J(l_{ri})$ is given by (38) evaluated at l_{ri}. Again, the treatment of the index i is treated in detail elsewhere [2, p. 45].

The TM rectangular magnetic field components H_x and H_y are evaluated according to

$$H_x(P) = J(l_{ri})\frac{x_2 - x_1}{\Delta C_r} \quad (42)$$

$$H_y(P) = J(l_{ri})\frac{y_2 - y_1}{\Delta C_r} \quad (43)$$

where $J(l_{ri})$ is evaluated as described for (41), while (x_1, y_1) and (x_2, y_2) are pairs of rectangular coordinates locating the ends of the rth contour subdivision. Again, it is the rth subdivision to which point P is in proximity. If point P is at the center of a contour subdivision, then $H_x(P)$ and $H_y(P)$ are each taken to be the average of H_x and H_y evaluated at the centers of the adjacent half subdivisions.

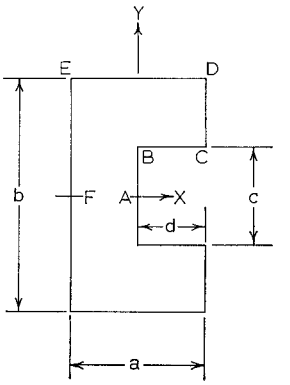

Fig. 7. Single-ridge waveguide cross section.

VIII. Example—Ridge Waveguide

The accuracy of the method presented here has been verified on computations of cutoff wave numbers, wall currents, and modal field distributions of the first several modes in rectangular and circular waveguides [2, pp. 47–70]. The high degree of accuracy inherent in this method will be discussed in Section IX.

In this section computed values of cutoff wave numbers, wall currents, and modal field distributions are presented for modes of the ridge waveguide shown in Fig. 7. In all computations presented, the waveguide has been subdivided so that

$$\frac{\Delta C}{\lambda} \leq 0.15 \quad (44)$$

where ΔC is the length of the longest straight-line segment used in the waveguide contour representations.

A. Cutoff Wave Numbers

Exact solutions for the single-ridge waveguide in Fig. 7 are not known. For this reason, values of cutoff wave numbers computed by the method developed here are compared to other estimates of the exact cutoff wave number. Values tabulated in Table II correspond to the waveguide in Fig. 7, with dimensions in the proportion $a:b:c:d = 2:4:2:1$. The values computed by the method developed here are believed accurate to within an error of 1 percent compared to exact values.

B. Wall Currents

For the single-ridge waveguide shown in Fig. 7 with dimensions in the proportion $a:b:c:d = 2:4:2:1$, the computed wall currents for the dominant waveguide mode and the lowest order TM mode are shown in Fig.

TABLE II
NORMALIZED CUTOFF WAVE NUMBERS (kb) FOR THE SINGLE-RIDGE WAVEGUIDE

Matrix Order	Mode	Wave Number (kb) Computed	Wave Number (kb) Reference	Percent Difference	Reference [16] Wave Number	Percent Difference	Reference [19] Wave Number	Percent Difference
13	TE^{odd}	2.2566	2.250[a]	0.31	2.2627	0.27	2.2412	0.68
15	TE^{even}	4.9373	4.8404[b]	2.0	4.9251	0.25	4.8460	1.9
13	TE^{odd}	6.5218	6.4575[b]	0.99	6.4864	0.54	6.4532	1.0
22	TE^{even}	7.5361	7.5074[b]	0.38	7.5249	0.15	7.5188	0.23
29	TM^{even}	12.164	11.974[b]	1.6			12.1416	0.18

[a] Value given in [9, p. 281] and [17].
[b] Value given in [18].

8. The values are plotted versus the distance around the waveguide contour $ABCDEF$ shown in the inset and were computed for matrices of orders shown in Table II, corresponding to each mode. In Fig. 8(a) the values are normalized with respect to the maximum value on the waveguide. In Fig. 8(b) the values were normalized with respect to the second largest current value on the waveguide. This scheme was chosen because the largest current value at point B is expected to be much larger than other values on the waveguide. It is known [8] that the transverse field components for either TM or TE modes become large near a waveguide corner with an internal angle greater than 180°.

C. Modal Fields

In Fig. 9 the distribution is given for the longitudinal field component of the dominant mode in the ridge waveguide treated in the previous two sections. The computed values are normalized with respect to the maximum value of field component over the cross section. The values shown in Fig. 9 are plotted over the shaded portion of the figure inset.

From field computations for rectangular and circular waveguide modes, it was observed that erratic accuracy was obtained at field points within less than one-fourth of a segment from the wall. For TE modes, the approximation of the charge distribution by pulses is expected to introduce somewhat greater error in values of electric field computed at points near the wall. However, at this time it is not known whether the formulation used is inappropriate for computation at such points or whether an error exists in the implementation of this formulation. Note that for TM modes in an arbitrarily shaped waveguide, the E_z component is known to be exactly zero at the wall, thus enabling a simple interpolation using the values determined more accurately at points greater than one-fourth of a segment from the wall.

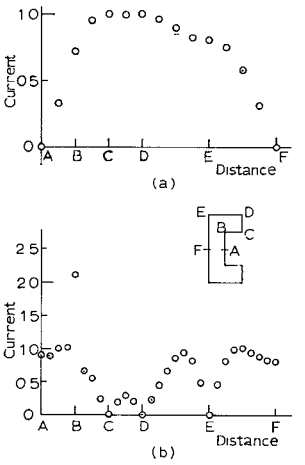

Fig. 8. Ridge waveguide wall currents. (a) TE^{odd}, $kb \approx 2.2$. (b) TE^{even}, $kb \approx 12$.

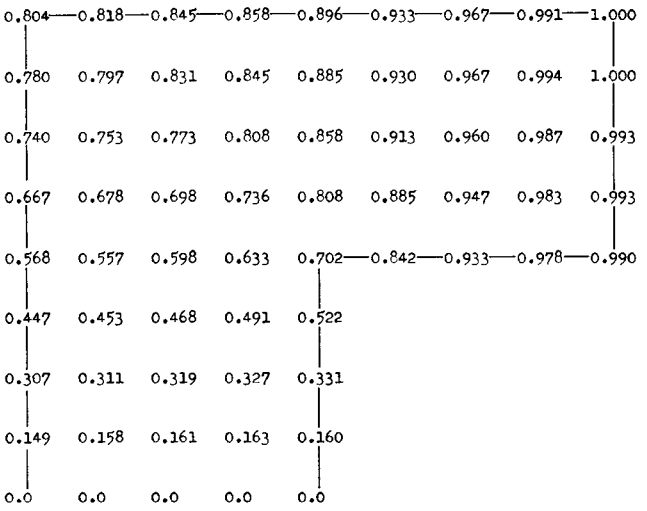

Fig. 9. Longitudinal field component for the dominant mode in a single-ridge waveguide.

IX. CONCLUSIONS

Six criteria are used here to assess the usefulness of available methods for solving the problem of the arbitrarily shaped waveguide. They are the following.

1) The effectiveness of the method for waveguides of different shapes.

2) The adaptability of the method to implementation by computer program.

3) The ability of the method to compute the first several modes in addition to the dominant mode.

4) The ability of the method to compute field distributions as well as cutoff wave numbers.

5) The accuracy of the method.

6) The availability of the method in the form of a working computer program.

The first five of these criteria were in essence established by Davies [1] and will be considered first here.

Finite difference solutions [9], [10] are hampered by slower convergence on waveguides with curved boundaries. This is due to the difficulty in imposing the problem boundary conditions. Furthermore, since higher order modes are obtained in an iterative process, good initial starts are necessary.

Point matching methods [11], [12] lose effectiveness for waveguides of complicated shape. In particular for reentrant regions, the usefulness of these methods seems questionable.

A segment matching solution [13] used polynomials which satisfy the boundary conditions as factors in the expansion functions; hence each waveguide solution becomes a separate problem.

Conformal mapping methods [14] require a transformation of the waveguide shape that is dependent upon the particular waveguide problem to be solved. Hence each waveguide becomes a separate problem and general implementation by computer program is difficult. Furthermore, the transformation required is known explicitly for few cases and the approximation of this transformation causes the effectiveness of the method to suffer for a variety of waveguide shapes.

Methods using polynominal expansion functions [15], [16] present the problem of choosing the order of the polynomials. Also, for reentrant shapes the determination of transverse field distributions becomes more difficult.

The method developed in this work has been demonstrated as satisfying the first five criteria above. Using relatively low-order matrices, cutoff wave numbers are determined to within a few tenths of a percent of exact values, while computed distributions of both longitudinal and transverse field components agree to within a few percent of exact values. Furthermore, the method developed here has been implemented by general computer programs listed and described elsewhere [2, pp. 98–110].

The chief limitations of the method developed here are as follows. The computation time for the determination of cutoff wave numbers can become substantial for higher order modes. Secondly, the field values at points within a quarter segment from the waveguide wall are computed less accurately than values at points further away.

References

[1] J. B. Davies, "Numerical solution of the hollow waveguide problem," presented at the XVIth General Assembly of URSI, Ottawa, Ont., Canada, Aug. 1969.

[2] B. E. Spielman, "Waveguides of arbitrary cross section by solution of a nonlinear integral eigenvalue equation," Ph.D. dissertation, Dep. Elec. Eng., Syracuse Univ., Syracuse, N. Y., Feb. 1971.

[3] R. F. Harrington, *Field Computation by Moment Methods*. New York: Macmillan, 1968.

[4] ——, "Matrix methods for field problems," *Proc. IEEE*, vol. 55, pp. 136–149, Feb. 1967.

[5] F. B. Hildebrand, *Methods of Applied Mathematics*, 2nd ed. Englewood Cliffs, N. J.: Prentice-Hall, 1965, pp. 12–13.

[6] V. N. Faddeeva, *Computational Methods of Linear Algebra*. New York: Dover, 1959, pp. 72–75.

[7] J. Ortega, "The Givens–Householder method for symmetric matrices," in *Mathematical Methods for Digital Computers*, vol. II, A. Ralston and H. S. Wilf, Eds. New York: Wiley, 1968, pp. 94–115.

[8] J. K. Reid and J. E. Walsh, "An elliptic eigenvalue problem for a reentrant region," *J. Soc. Indust. Appl. Math.*, vol. 13, pp. 837–850, Sept. 1965.

[9] J. B. Davies and C. A. Muilwyk, "Numerical solution of uniform hollow waveguides with boundaries of arbitrary shape," *Proc. Inst. Elec. Eng.*, vol. 113, pp. 277–284, Feb. 1966.

[10] C. H. Tang and Y. T. Lo, "Numerical analysis of the eigenvalue problem of waves in cylindrical waveguides," Antenna Lab., Univ. Illinois, Urbana, Tech. Rep. 45, Mar. 1960.

[11] H. Y. Yee and N. F. Audeh, "Uniform waveguides with arbitrary cross-section considered by the point-matching method," *IEEE Trans. Microwave Theory Tech. (1965 Symposium Issue)*, vol. MTT-13, pp. 847–851, Nov. 1965.

[12] R. H. T. Bates, "The theory of the point-matching method for perfectly conducting waveguides and transmission lines," *IEEE Trans. Microwave Theory Tech.*, vol. MTT-17, pp. 294–301, June 1969.

[13] P. A. Laura, "A simple method for the determination of cutoff frequencies of waveguides with arbitrary cross sections," *Proc. IEEE* (Lett.), vol. 54, pp. 1495–1497, Oct. 1968.

[14] H. H. Meinke, K. P. Lange, and J. F. Ruger, "TE- and TM-waves in waveguides of very general cross section," *Proc. IEEE*, vol. 51, pp. 1436–1443, Nov. 1963.

[15] P. Silvester, "A general high-order finite-element waveguide analysis program," *IEEE Trans. Microwave Theory Tech.*, vol. MTT-17, pp. 204–210, Apr. 1969.

[16] R. M. Bulley and J. B. Davies, "Computation of approximate polynomial solutions to TE modes in an arbitrarily shaped waveguide," *IEEE Trans. Microwave Theory Tech.*, vol. MTT-17, pp. 440–446, Aug. 1969.

[17] T. S. Saad, Ed., *The Microwave Engineers' Handbook and Buyers' Guide*. Dedham, Mass.: Horizon House, 1965, p. 57.

[18] T. W. Bristol, "Waveguides of arbitrary cross section by moment methods," Ph.D. dissertation, Dep. Elec. Eng., Syracuse Univ., Syracuse, N. Y., Nov. 1967, pp. 90–91.

[19] M. J. Beaubein and A. Wexler, "Unequal-arm finite-difference operators in the positive-definite successive overrelaxation (PDSOR) algorithm," *IEEE Trans. Microwave Theory Tech. (1970 Symposium Issue)*, vol. MTT-18, pp. 1132–1149, Dec. 1970.